

Article

Tectonic-Paleoseismological Characteristics and Quaternary Activity of Maymundağı Fault (Northern Acıgöl Graben)

Şahali Kaya * and Mete Hançer

Department of Geological Engineering, Faculty of Engineering, Pamukkale University, Kinikli, Denizli 20160, Turkey; mhancer@pau.edu.tr

* Correspondence: sahalikaya@hotmail.com

Abstract: The Aegean region and its graben system constitute one of Turkey's most significant seismic zones. The faults within the Aegean graben generate numerous earthquakes, leading to various human and economic losses. To better understand the seismicity of western Anatolia, it is necessary to obtain concrete findings regarding the seismic history of earthquake-producing graben faults. This can be achieved through paleoseismological studies and other relevant disciplines. This study focuses on paleoseismological investigations along the northern boundary fault of the Acıgöl graben, located east of the Aegean graben system. The Maymundağı fault zone has been examined in two separate segments: east and west. The Dazkırı segment to the east shows evidence of movement dating back at least 10,000 years, with subsequent intensified activity observed later on the western Bozkurt segment. An earthquake occurred approximately 2370 years ago east of the Bozkurt segment, followed by movements migrating westward, resulting in earthquakes approximately 1322 and 598 years ago. Further analysis of the western segment indicates an average recurrence interval of 724 years for earthquakes, with a slip rate of 0.58 mm/year. Based on these findings, a future earthquake can be expected in this region around 2028–2129 AD.

Keywords: Acıgöl graben; Maymundağı fault; Dazkırı fault segment; Bozkurt fault segment; paleoseismology; earthquake



Citation: Kaya, Ş.; Hançer, M. Tectonic-Paleoseismological Characteristics and Quaternary Activity of Maymundağı Fault (Northern Acıgöl Graben). *Appl. Sci.* **2024**, *14*, 8852. <https://doi.org/10.3390/app14198852>

Academic Editor: Roberto Scarpa

Received: 27 July 2024

Revised: 17 September 2024

Accepted: 23 September 2024

Published: 1 October 2024



Copyright: © 2024 by the authors. Licensee MDPI, Basel, Switzerland. This article is an open access article distributed under the terms and conditions of the Creative Commons Attribution (CC BY) license (<https://creativecommons.org/licenses/by/4.0/>).

1. Introduction

Denizli, a key city in Turkey's textile and travertine industries, is one of the most significant urban centers in both Turkey and the Aegean Region, with a population exceeding one million. The Aegean region, encompassing the graben system, constitutes one of Turkey's most significant seismic zones. The faults within the Aegean graben generate numerous earthquakes, leading to various human and economic losses. Historical records document several major instrumental earthquakes in the region, including the 1899 Menderes earthquakes ($M = 6.5$ and 7.1), the 1956 Söke-Balat earthquake ($M = 6.8$), the 1965 Denizli earthquake ($M = 5.7$), the 1969 Alaşehir earthquake ($M = 6.7$), and the 1970 Gediz earthquake ($M = 7.2$). The Acıgöl basin forms the approximate eastern boundary of the Aegean graben system in southwestern Anatolia.

This region is characterized by rapid deformation and seismic activity due to dominant graben structures, including numerous small grabens in various orientations and larger east–west trending grabens. During the Late Oligocene to Early Miocene, the region experienced significant continental extension. This extension led to the formation of prominent morphological structures, such as the Gediz-Alaşehir graben (GAG) and the Büyük Menderes graben (BMG) (Figure 1). These structures have been extensively studied by researchers [1–5]. The east–west trending graben border faults are seismically active [6–12].

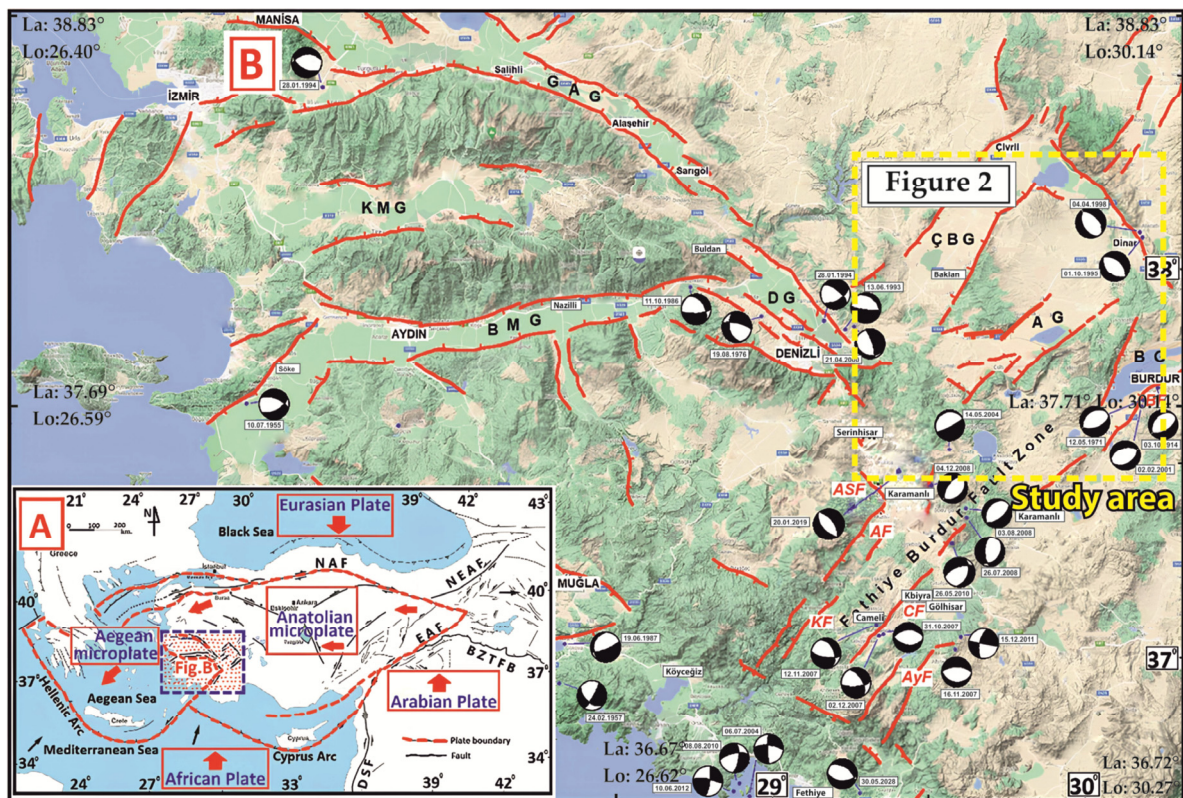


Figure 1. (A) Location map in the tectonic framework of Turkey, annotations: NAF: North Anatolian Fault, EAF: East Anatolian Fault, NEAF: Northeast Anatolian Fault, BZTFB: Bitlis-Zagros Thrust and Fold Belt (modified from [13–16]), (B) morphotectonic map of historical seismic faults and focal mechanisms in southwestern Anatolia [17] (via Google Maps). Annotations: BMG: Büyük Menderes graben, KMG: Küçük Menderes graben, GAG: Gediz-Alaşehir graben, DG: Denizli graben, ÇBG: Çivril-Baklan graben, AG: Acıgöl graben, BG: Burdur graben, ASF: Acıpayam-Serinhisar Fault, AF: Acıpayam Fault, BF: Burdur Fault, AyF: Altınyayla Fault, KF: Kelekçi Fault, CF: Çameli Fault (adapted from [5,16,18]).

The formation of east–west trending grabens remains a subject of debate among researchers. Some argue that these grabens began to form during the Tortonian (Upper Miocene) [19], while others suggest that they originated in the Early Miocene and have continued to evolve up to the present [20,21]. Recent studies, however, indicate that Miocene sediments are not associated with the present-day grabens and propose that the development of east–west grabens occurred 5 million years ago (Plio-Quaternary) due to north–south extension [22]. In the eastern Aegean, NE–SW directional opening and, accordingly, NW–SE directional grabens/graben edge faults are active. These include the eastern part of the GAG, the Denizli graben (DG), the Dinar fault, and the Acıpayam-Serinhisar fault [16]. The fault systems that form NW–SE trending grabens or graben-bounding faults are also active among others [23,24], as evidenced by the 1965 Denizli earthquake ($M = 5.7$) and the 1995 Dinar earthquake ($M = 5.7$).

In western Anatolia, NE–SW trending basins and the elevations between them are secondary prominent tectonic features (e.g., Gediz, Simav, Gördes, Demirci, Selendi, and Uşak-Güre basins). Particularly towards the east, NE–SW trending basins become more pronounced, including the Çivril-Baklan graben (ÇBG), the Acıgöl graben (AG), and the Burdur graben (BG). Active faults forming grabens in this trend were highlighted by the 1914 Burdur earthquake ($M = 7.0$) and the 1971 Burdur earthquake ($M = 5.9$). Among these, the ÇBG in the NW and the BG in the SE predominantly trend NE–SW. The AG lies between them, trending NE–SW to the east and transitioning to an E–W trend towards the west. The

2019 Bozkurt earthquake ($M = 6.0$) occurred along the western E-W trending fault of the Acıgöl depression, as inferred from fault-plane solution mechanisms [25] (Figure 2).

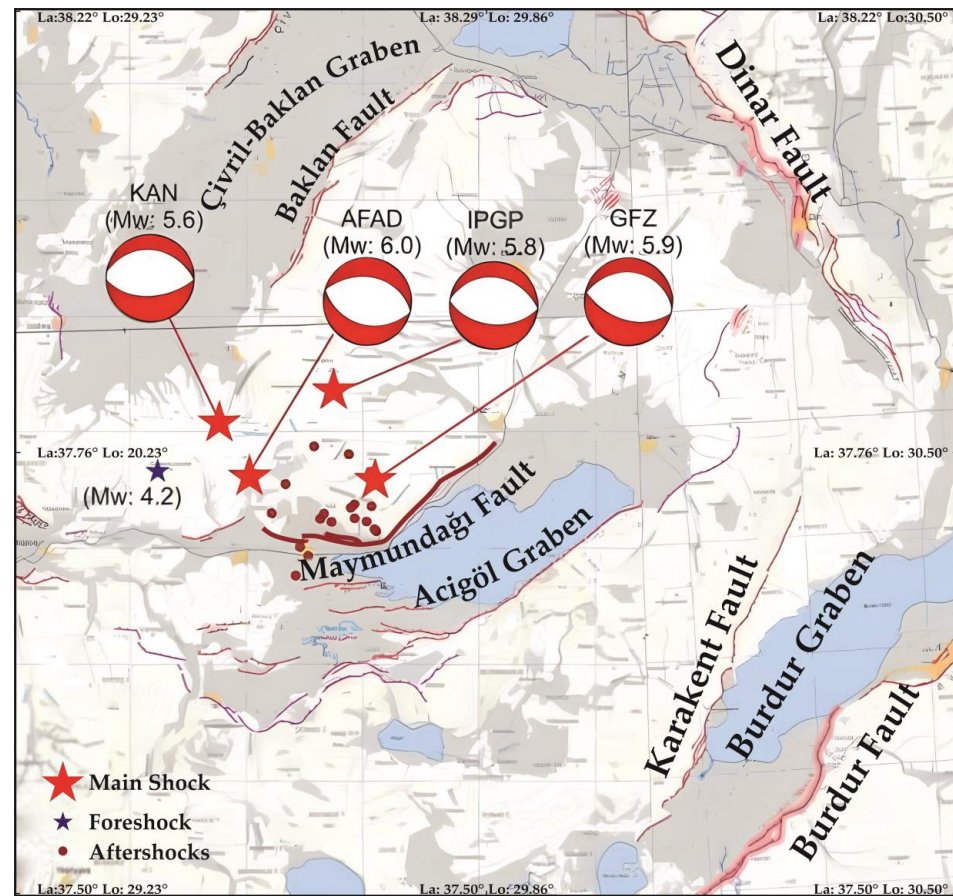


Figure 2. 1/250,000 active fault map showing precursor, main shock, and aftershocks of the 8 August Denizli Bozkurt earthquake [26]. Abbreviations: KAN: B.U. Kandilli Observatory and Earthquake Research Institute; AFAD: Disaster and Emergency Management Authority of Turkey; GFZ: German Research Centre for Geosciences; IPGP: Institute of Earth Physics, Paris (modified from [25]).

In this context, tangible data regarding the seismic history of the edge faults that form the Acıgöl graben will make significant contributions to the literature in terms of the seismicity of the region. Additionally, the region's proximity to major settlements such as Denizli, Burdur, and Afyon, coupled with western Anatolia's importance in terms of industry and tourism, enhances the significance of this contribution. Thus, the data obtained from this study will provide valuable guidance for settlement planning, zoning, and urbanization. In addition to all this, western Anatolia graben structures are not only regional but also global structures. Understanding the crustal opening in western Anatolia will contribute to Anatolian tectonics and the seismicity of SW Europe. As a result, the potential damage and loss of life from future earthquakes can be minimized. Therefore, investigating the seismic history of the region has been the focus of this study.

2. Geological-Tectonic Setting

The base blocks of faults bounding the CBG, AG, BG, and depression areas contain autochthonous Beydağları, Lycian nappes, and molasse-type rock units. South of the Acıgöl depression, the study area includes Mesozoic-aged limestone, dolomitic, and ophiolitic mélangé units, while to the north of the basin, Oligocene-aged marine conglomerates, classified as molasse-type sediments, are found, forming the elevations of the basin. In the depression areas, Neogene-aged sediments and younger Quaternary units are present.

Neogene-aged sediments consist of lacustrine sediments and continental alluvial fan deposits [27–30] (Figure 3).

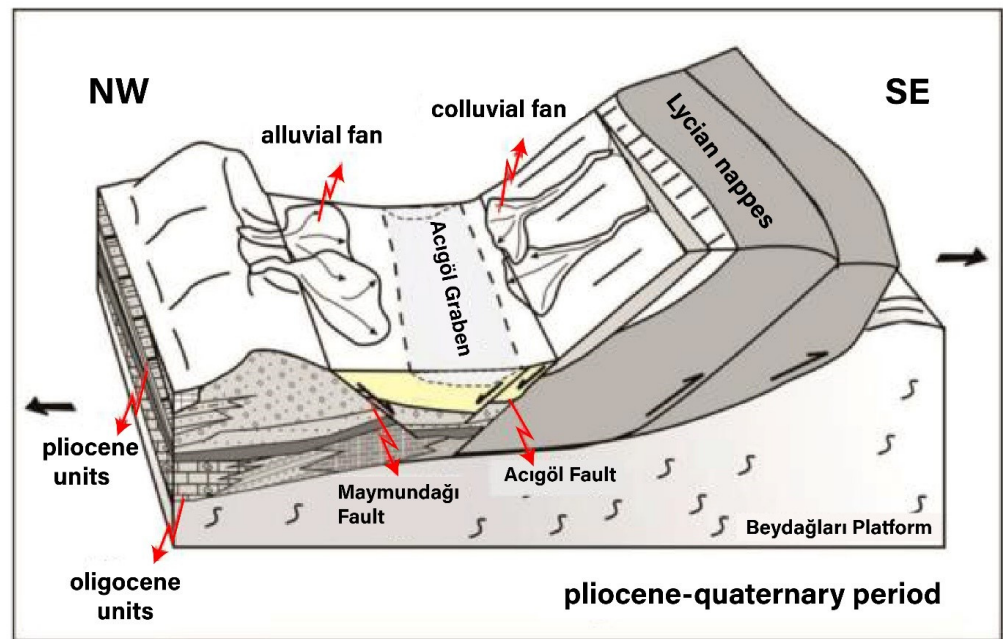


Figure 3. Block diagram depicting the present-day model of the study area showing the Pliocene-Quaternary period (modified from [30]).

The Acıgöl depression covers an area of 150 km² and is generally characterized as a region that is 30 km long and 10 km wide, trending mainly NE-SW in the east and E-W in the west. In this context, the geological-tectonic structure of Acıgöl graben and its surroundings are shown below (Figure 4). The formation of the Acıgöl depression involved the deposition of lacustrine sediments stored in a narrower central area due to the basin's renewed subsidence after early Pliocene moist climatic conditions. The Acıgöl basin is a closed graben type depression limited by faults, primarily accumulating sediments controlled by NE strike direction faults [27]. The Acıgöl graben, similar to other regions in southwestern Turkey, is a structure that developed in two stages (episodic development), comprising two unconformably separated fills or two separate fills [31–34]. The older rocks in the Acıgöl graben have undergone deformation (folded, reverse, and strike-slip faults), containing records of both the opening regime controlling the graben during its initial formation (first-stage extensional tectonic regime) and the compressional regime that terminated the graben formation during the first stage and subsequently deformed it [33].

The Acıgöl graben is separated from the Burdur graben to the south by the Söğütadağı-Tınazdağı horsts. A young graben of Pliocene-Quaternary age, located at higher elevations between the Söğütadağı and Tınazdağı horsts and the other two grabens, has been identified and named the Akgöl graben. The faults of this graben are considered the source of the 1971 Burdur earthquake ($M = 5.9$) [35,36]. Historical earthquake data is crucial for assessing the hazard risk in the region. In this study, trench excavations were conducted at three different points along the Maymundağı fault zone to perform paleoseismological investigations. The aim of the study was to trace evidence of earthquakes over the past few thousand years, and the excavations were mapped (Figure 5). Samples taken from within the trenches were documented with C14 age analysis. All these data are presented under separate trench headings below.

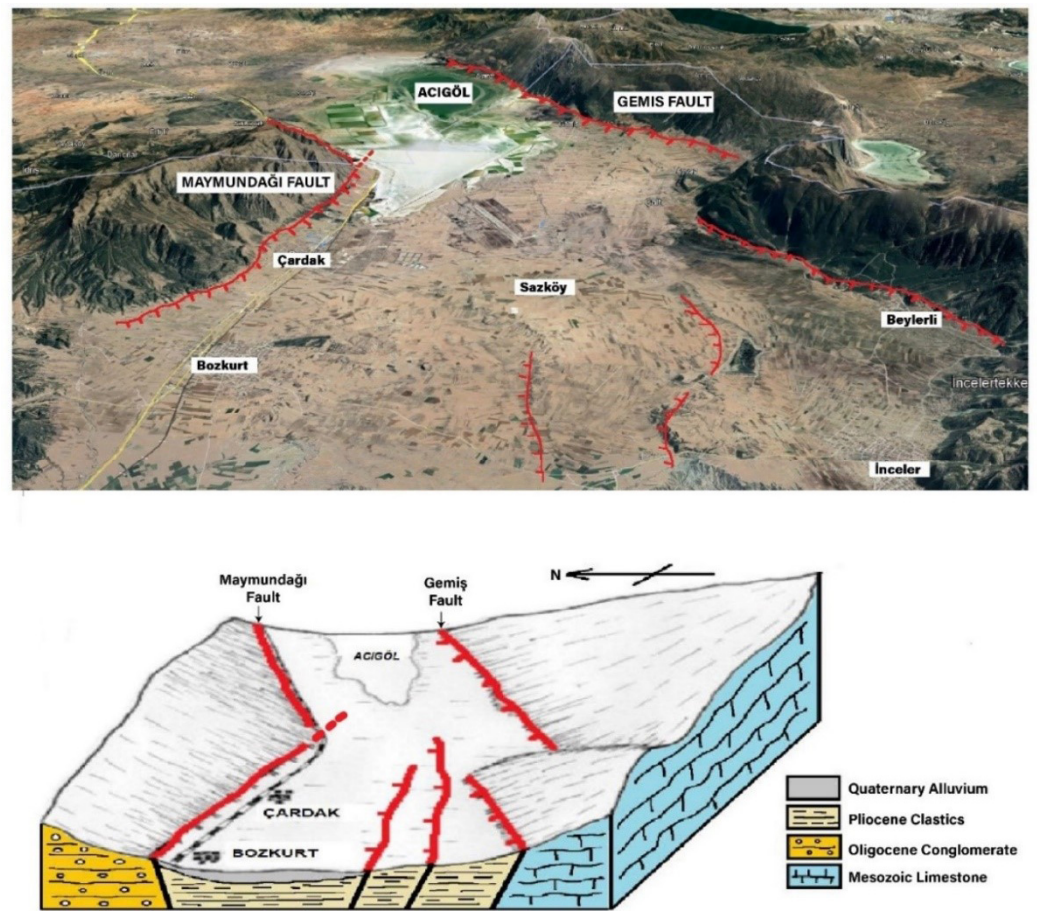


Figure 4. Generalized photograph and block diagram showing the geological-tectonic structure of the Acıgöl graben and its surroundings (scale not shown).

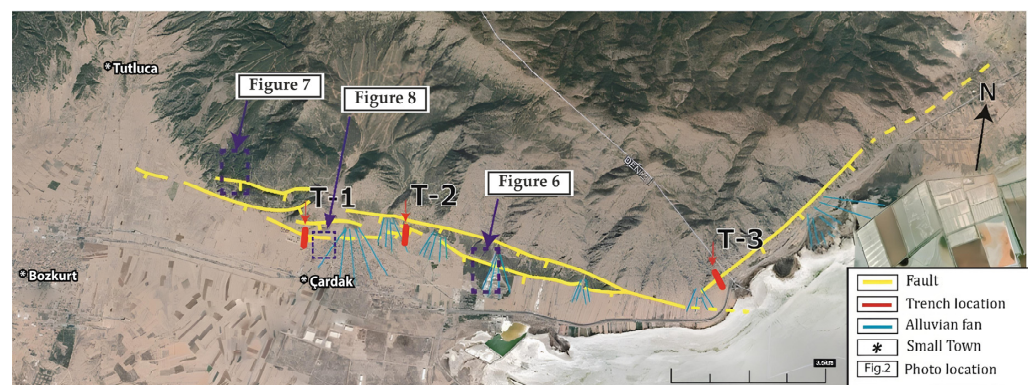


Figure 5. Active fault map showing the general position of the Maymundağı fault on the northern side of the Acıgöl graben (Adapted from [37]), indicating the locations of shapes and trenches.

2.1. Maymundağı Fault

The Maymundağı Fault, which forms the northern boundary of the Acıgöl depression, is a predominantly normal fault with a minor right-oblique component, extending 30 km in length. The fault is divided into two separate segments: the Dazkırı segment, 13 km long and dipping to the southeast in a NE direction, located in the east, and the Bozkurt segment, 17 km long and dipping to the south in an E-W direction, situated in the west. This fault zone extends approximately NE-SW direction from Dazkırı settlement in the

east to Çardak in the west, covering a distance of 13 km. Westward from Çardak, the fault zone changes to an approximately E-W orientation and terminates north of the Çardak settlement. Approximately 300 m north of this line is a synthetic fault with a length of about 4.5 km (Figure 5). The westward continuation of the fault zone west of Çardak leaps 300 m southward and continues for 4 km. These segments are marked as active faults on the active fault map.

The base blocks in the field of the active fault zone located in the northern part of the area contain fundamental units. These units are mostly composed of Oligocene-aged conglomerate units. In the base block south of the fault, younger units such as slope debris, fan deposits, and alluvium are present. The Maymundağı fault zone north of Çardak forms a boundary with Oligocene-aged conglomerates and other younger units [30], indicating that the Acıgöl graben is a semi-symmetric graben, and the northern Maymundağı fault (Çardak fault) is a vertically downthrown fault (Figure 3).

A geography-oriented study to determine morphological features using GIS [38] emphasized that the Baklan graben formed earlier north of the mountain and the Acıgöl graben formed more recently, with hooked drainage networks developing within the basin due to faulting. Additionally, the researchers highlighted less tectonic activity in the northeast of the fault, contrasting with higher activity in the southern and southeastern sectors of the Maymundağı fault.

2.1.1. Geometry and Segment Structure of Maymundağı Fault

The Maymundağı fault zone continues along a N 50°E trend between east of Çardak and Dazkırı. The fault trace is clearly observed due to morphotectonic landforms north of Acıgöl. Large and thick fan deposits have developed in front of the fault (Figure 6). From Dazkırı to Çardak eastward, the Maymundağı fault follows a NE trend, changing its orientation westward from Çardak to approximately E-W, occasionally also N 70° E–N 80° E, and continues to the north of Çardak. Two parallel segments of the fault extend approximately 300 m apart (Figure 7).

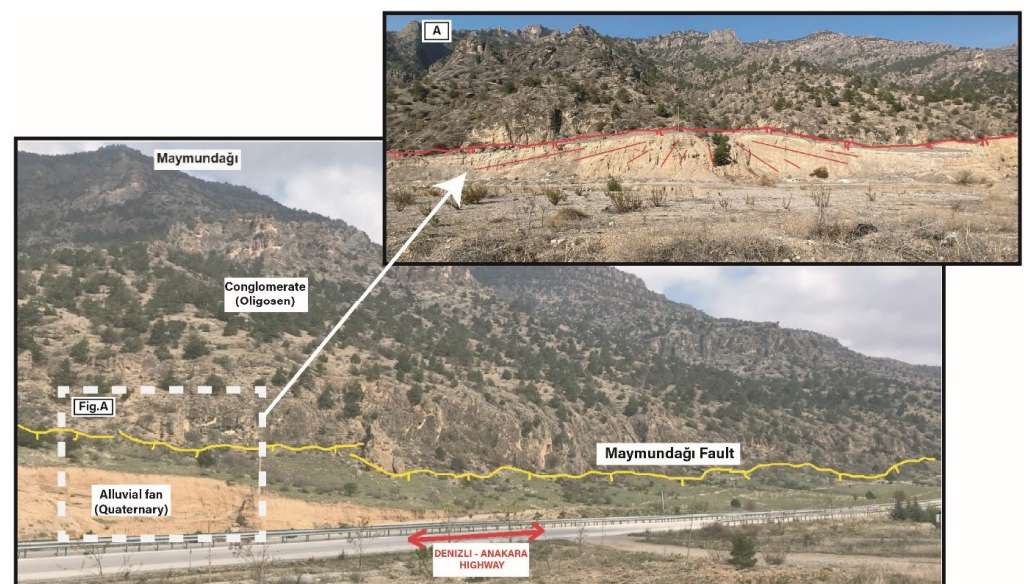


Figure 6. View of the Maymundağı fault on the east side of the Denizli-Ankara highway (looking towards NW) A: Fan deposits developing in front of the Maymundağı fault.

The northern segment of these faults is clearly observed to be 6 km long in field observations (Figure 8). The fault zone observed as a step-like feature (Figure 7) terminates westward at Çardak north and makes a southward jump continuing westward. The fault fractures observed in two separate segments north of Çardak are morphotectonically

distinct and particularly noticeable. The fault observed over a length of 600–700 m is not visible westward beyond the alluvium.

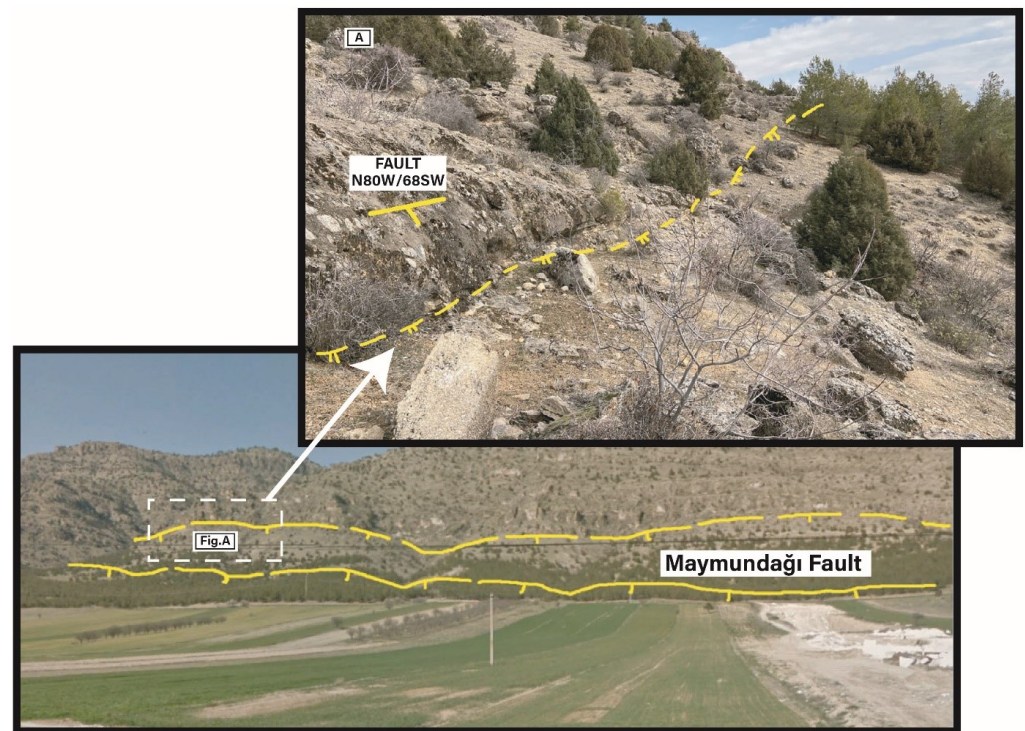


Figure 7. Appearance of the Maymundağı fault in two parallel segments at Çardak north in the NNE view. A: close-up view of the northern segment of the parallel segments (northern segment of the Maymundağı fault).

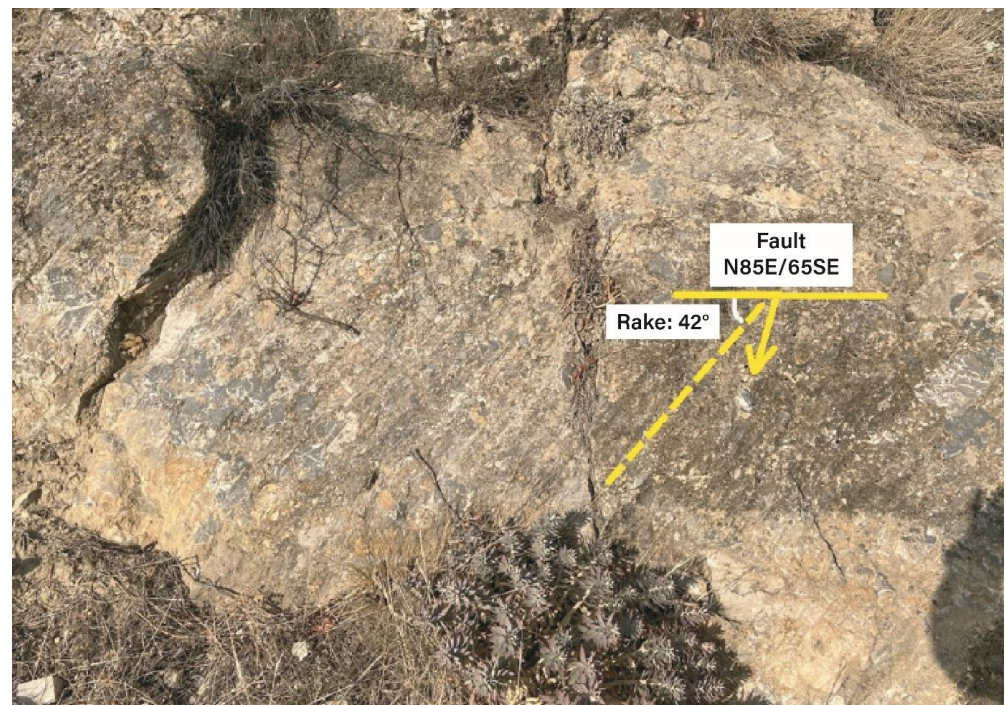


Figure 8. Fault plane and slickenlines observed on the road at the northern boundary of Çardak settlement (view towards north).

Slickenlines on the fault plane of the segment passing 250 m south of this fracture were observed (Figure 8). A fault with the N 85° E/65° SE location was detected on the road of the neighborhood at the northern border of the Çardak campus. The slickenline on this fault, which is a normal fault with a right oblique component, shows a rake angle of 42° (Figure 8).

The westward continuation of this fault was revealed in Trench #2, but its further westward continuation disappears in the alluvium. In general, the continuation of the fault zone towards the west continues with a jump of approximately 200 m to the north. The continuation of this jumping segment appeared in Trench #1 (See: Trench #1 and 2).

2.1.2. Paleoseismological Studies

Ref. [39] conducted paleoseismological studies on the Maymundağı fault, examining it in two separate sections: the Dazkırı and Bozkurt segments. The researchers noted that Quaternary-aged alluvial and colluvial fans are intermittently cut by the fault. Emphasizing an extensional regime in the NNW-SSE direction along the Maymundağı fault, they identified at least three earthquakes during the Late Quaternary-Holocene period on the Bozkurt segment that resulted in surface ruptures. However, they did not specify radiocarbon analysis results or earthquake dating. Another study conducted for paleoseismology west of the northern fault of the graben, the Maymundağı fault, by [40], involved OSL analysis in trench studies, indicating a total vertical throw of 850 m over 1.5 million years and an annual sediment accumulation rate of 0.6 mm. The researcher suggested that the Maymundağı Fault Zone might extend up to 50 km towards Dinar. It was noted that surface ruptures occurred in the Dazkırı region during the 1995 Dinar earthquake ($M = 6.1$).

Historical earthquake data is crucial for assessing the hazard risk in the region. In this study, trench excavations were carried out at three distinct locations along the Maymundağı fault zone to conduct paleoseismological investigations. The aim of the study was to trace evidence of earthquakes over the past few thousand years, and the excavations were documented (Figure 5). Samples taken from within the trenches were documented with C14 age analysis. All these data are presented under separate trench headings below.

2.1.3. Trench-1 (T-1)

Initially, at a suitable geological-topographical location along the westward extension of the Bozkurt segment of the Maymundağı fault zone, which forms the northern boundary of the Acıgöl (Denizli-Afyon) graben basin, Trench-1 (T-1) was excavated. This trench was opened near Toki residential buildings west of the Çardak district in Denizli Province, where morphotectonic features are prominently visible, oriented along N 10° E direction, with a length of 15 m, focusing on the SE wall of the trench. The NE end of the trench is located at coordinates 37.831787°, 29.660847°, and the SW end is at 37.831629°, 29.660874° (Figure 9).

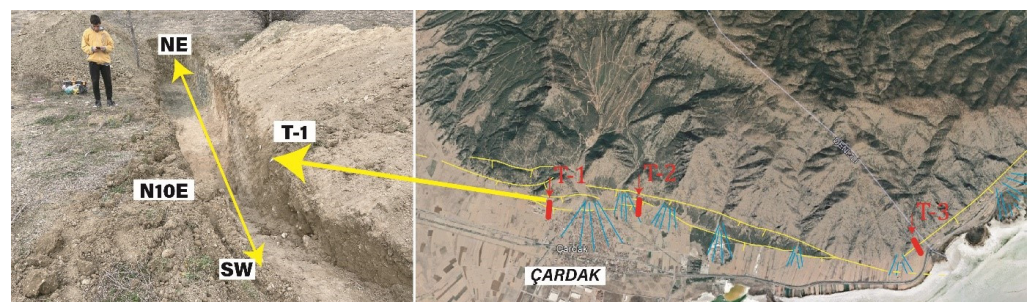


Figure 9. Location and route of Trench-1.

The stratigraphy within Trench-1, predominantly consisting of slope debris and fan deposits, includes a lowermost unit (Unit A) of light brownish schist. Above this, towards the middle sections of the trench, rocks composed mainly of ophiolitic components (Unit B)

and altered weathered ophiolite unit rocks (Unit C) are found. These units are overlain by brownish-yellow sands (Unit F). Between 7 and 11 m from the NE, a firm white clay gravel unit (Unit D) at the base level is covered by brownish-yellow sands and gray clay gravel blocks (Unit E) towards the SE. Thicker layers of brown block gravelly clay unit (Unit G), likely younger, overlay towards the SE. The uppermost layer consists of natural soil (Unit I) (Figure 10).

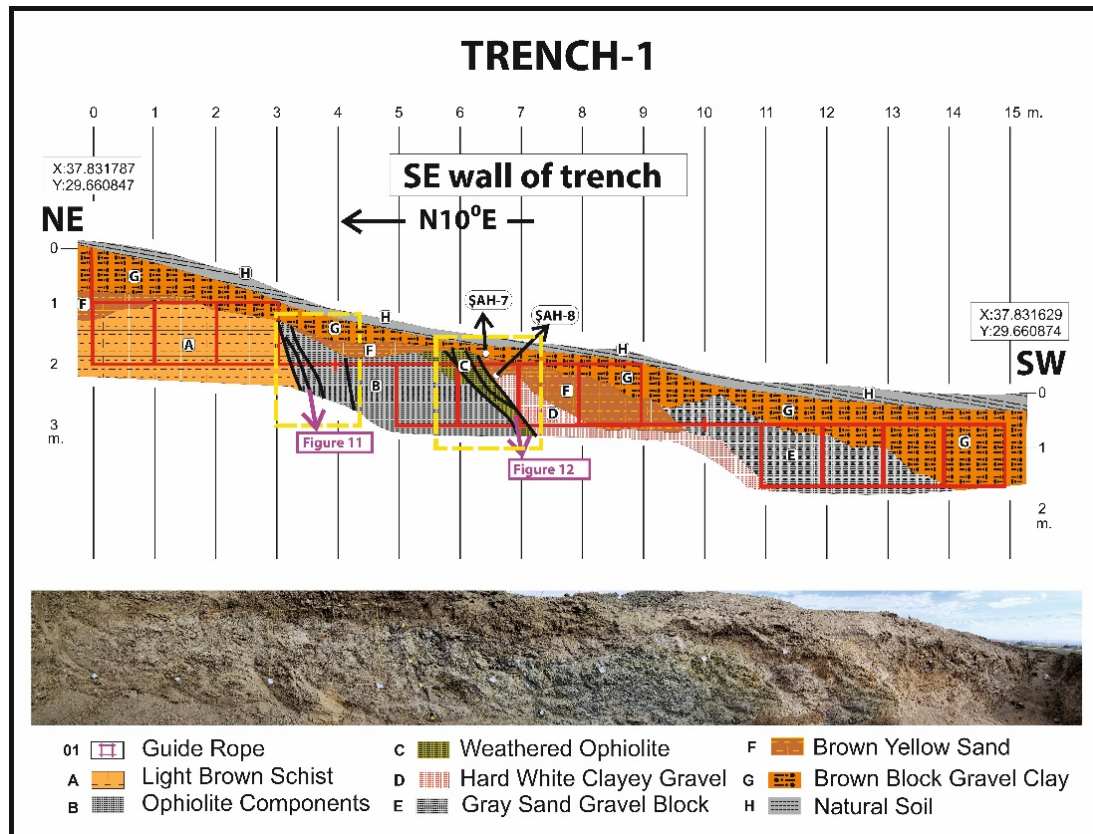


Figure 10. View of Trench-1 and the geological cross section on the SE wall of the trench (explanations of the geological units and faults are in text) [41].

Between 3 and 5 m from the northeast in Trench-1 (Figure 11), small throw fault planes dominated by an average E-W orientation and dipping about 70 to 85 degrees towards the south were observed. Another fault zone was observed between 6 and 7 m from the northeast in the same trench (Figure 12), characterized as a primary fault due to significant fault throw and intense weathering, with a measured orientation of N80° E/70° SE. The date of the radiocarbon sample taken at the base level of the brown block pebble and stony clay unit covering these faults is 598 ± 22 years (ŞAH-7). The calendar age is 1168–1263 AD. There is a brown-yellow sand level beneath this unit, which is intersected by the fault zone but also overlies the older lithologies below. The date of the radiocarbon sample taken from the base level of this unit is 1322 ± 22 years (ŞAH-8). The calendar age is 655–774 AD. Thus, this fault zone is interpreted to have generated surface ruptures in two separate periods of earthquake activity. The fault throw between the top and base blocks of the brownish-yellow sand level was measured to be approximately 42 cm (Figures 10–12). Detailed information is provided under the paleoseismological interpretation.

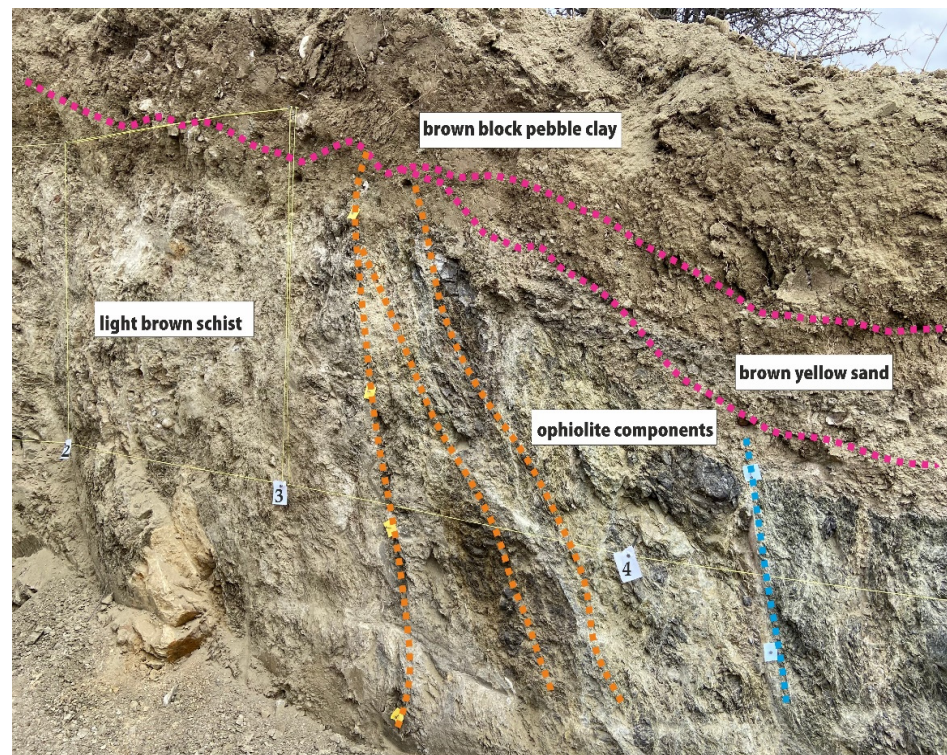


Figure 11. Section of Trench-1 between 3 and 5 m from the NE (view towards E-SE).

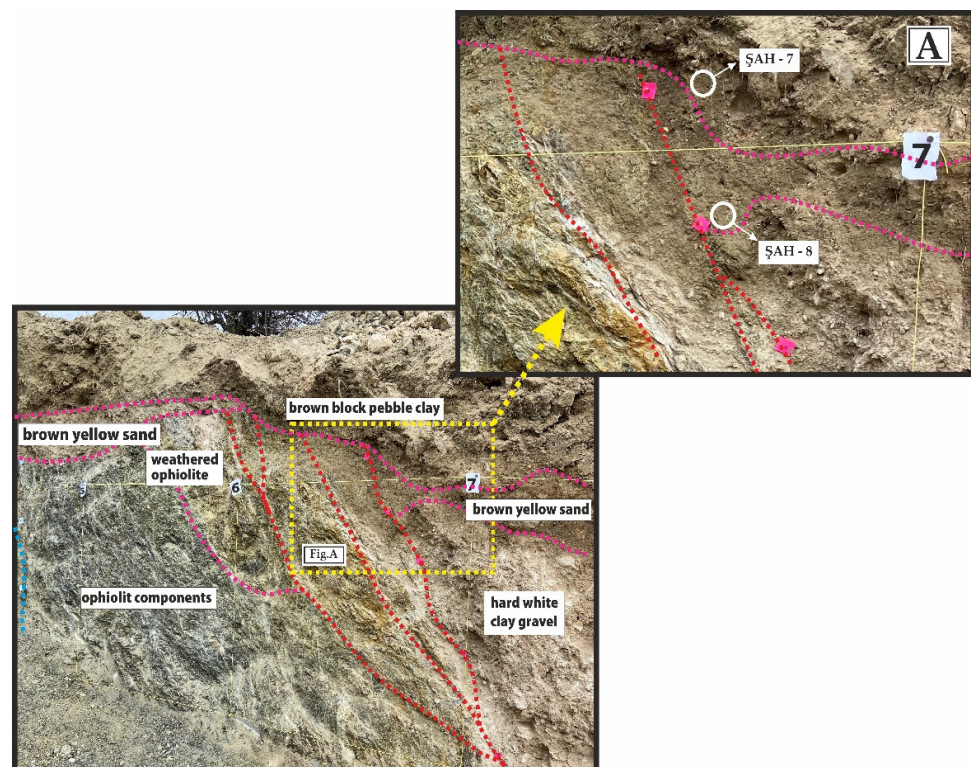


Figure 12. Section of Trench-1 between 5 and 7 m from the NE (view towards E-SE). A: Locations of samples taken for C14 dating, ŞAH-7 and ŞAH-8 samples.

2.1.4. Trench-2 (T-2)

About 2 km east of Trench-1 (T-1) along the same segment's eastern direction on the E-W oriented Bozkurt segment of the Maymundağı fault zone, Trench-2 (T-2) was excavated.

This trench was opened at a suitable geological-topographical location along the westward extension of the segment that forms the northern boundary of the Acıgöl (Denizli-Afyon) graben basin. The trench was opened northeast of Çardak district in Denizli province, where morphotectonic features are visible, oriented along N-S direction, with a length of 12 m focusing on the eastern wall of the trench. The N end of the trench is located at coordinates 37.834454°, 29.687342°, and the S end is at 37.844318°, 29.687349° (Figure 13).

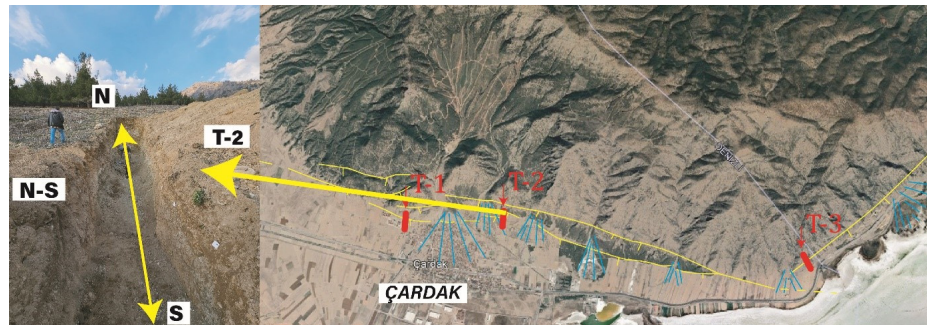


Figure 13. Location and route of Trench-2.

The stratigraphy within Trench-2, predominantly composed of slope debris lithologies, includes at the base a hard conglomerate sandstone unit (Unit A), which also constitutes the base block of the fault. In the upper block, there is a thinly bedded mudstone unit (Unit B). Further above, a reddish clay gravel unit (Unit D) extends inclinedly towards the end of the trench, occasionally reaching thicknesses of up to 2 m. Within the trench, between 8 m from the north, a large gray-white gravel unit (Unit C) disappears into the trench base. Between 4 and 10 m from the north, a brown gravelly clay unit (Unit F) overlies the reddish clay gravel unit. The uppermost unit is a white sand gravel unit (Unit E), which is comminuted in the last 2 m from the north. Natural soil (Unit G) is at the top (Figure 14).

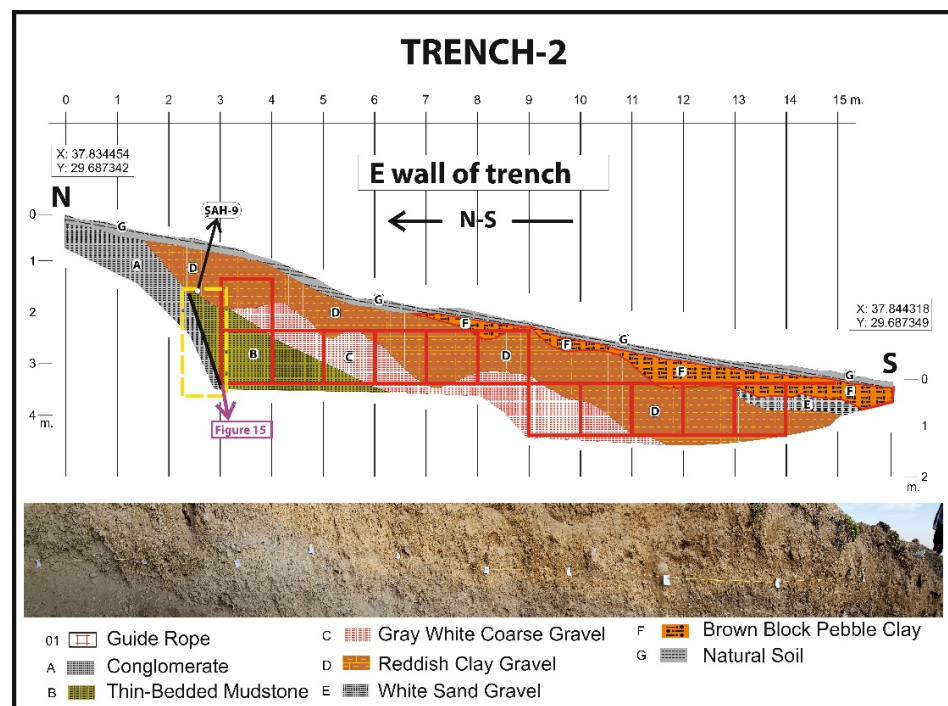


Figure 14. View of Trench-2 and the geological cross section on the E wall of the trench (explanations of the geological units and faults are in text).

Between 2 and 3 m from the north in Trench-2 (Figures 15 and 16), a fault plane was observed dipping southward. The main fault here was measured at a $N80^{\circ} E/75^{\circ} SE$ orientation. The date of the radiocarbon sample taken from the base level of the reddish clayey gravel unit covering this fault is 2370 ± 24 years (ŞAH-9). The calendar age is 517–392 BC. Detailed information is provided under the title of paleoseismological interpretation.

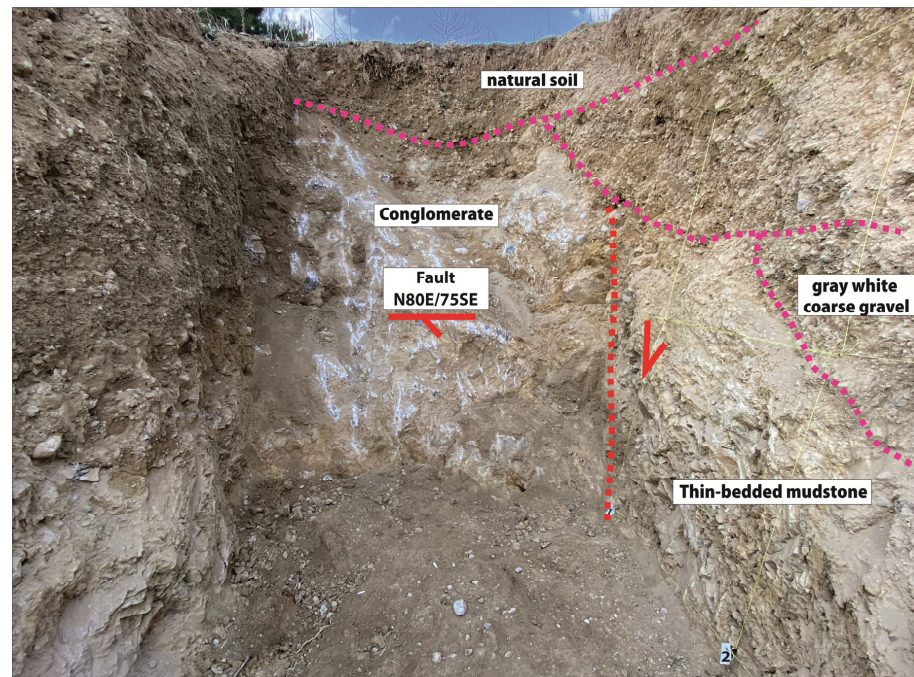


Figure 15. Fault mirror and lithological units observed at the northern end of Trench-2 (View towards N).

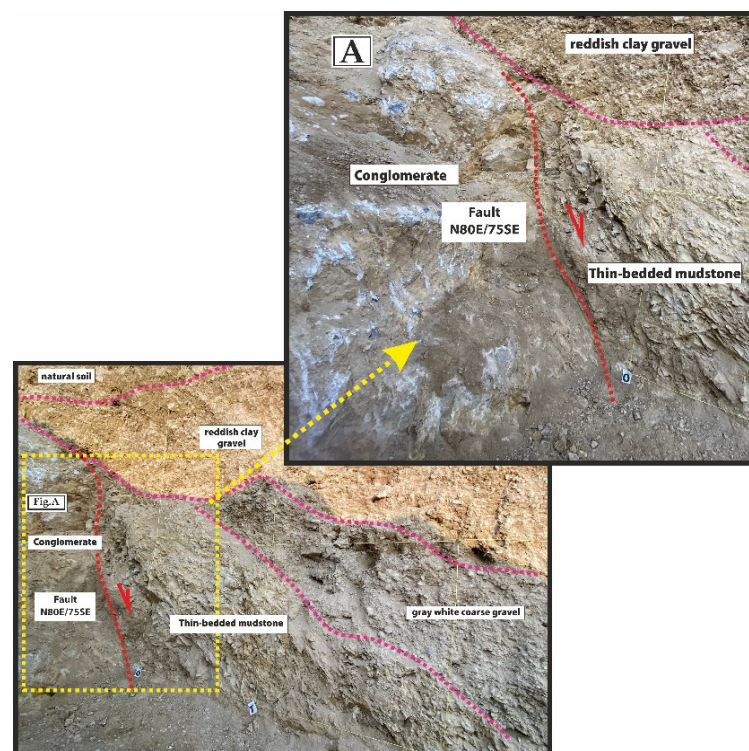


Figure 16. Lithological units between 0 and 2 m from K in Trench-2 (View towards NE). A: A close look at the slickens in trench 2.

2.1.5. Trench-3 (T-3)

Moving further east from Trench-2 along the E-W trending Bozkurt segment to the NE-SW trending Dazkırı segment, Trench-3 was located on the southwest flank of this segment. Trench-3 was opened where geological-topographical conditions were suitable, following the southwestern edge of the Maymundağı fault zone, which forms the northern boundary of the Acıgöl (Denizli-Afyon) graben basin (Figure 17). Morpho-tectonic traces were observed on the eastern side of Acıgöl, where Maymundağı changes from an east to west direction towards the northeast, meeting Oligocene-aged units and current sediments. At a prominent location where these traces intensified, a trench was excavated along the N 40 W direction, spanning 20 m, with the NE wall being investigated. The coordinates for the NW end are 37.830370° , 29.748604° , and for the SE end are 37.830246° , 29.748782° .

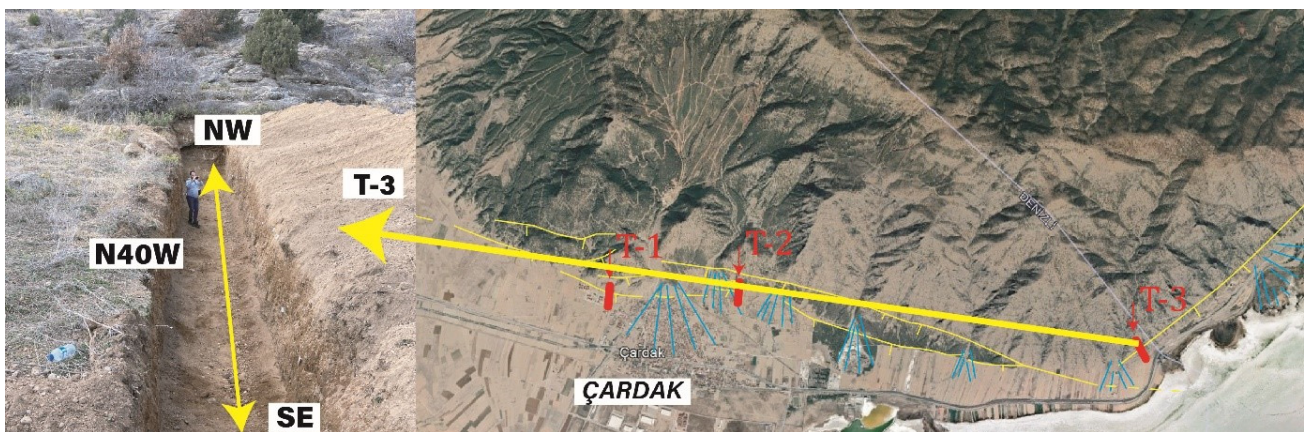


Figure 17. Location and route of Trench-3.

The trench stratigraphy is dominated by debris slope and alluvial fan lithologies. At the base, a hard-conglomerate sandstone unit outcrops and forms the base block of the fault (Unit A). Overlying this unit is a gravelly sand layer (Unit B), seen intermittently along the trench floor, defining the base level of the trench throughout its length. The fault's hanging wall includes a sparse gravelly clay unit (Unit C), while blocky gravel clay units (Unit D) are visible at various levels within the trench, reaching thicknesses of 10–15 cm. Further up, an open gray clay sand gravel unit (Unit E), covering both sides of the fault and observed along the trench, is present. The uppermost layer comprises natural soil (Unit F) (Figure 18).

Within Trench-3, at the northern end, a fault plane was observed overlying the conglomerate unit, dipping southeastward. The position of the main fault was measured as $N45^{\circ} E/50^{\circ} SE$ (Figure 19). The date of the radiocarbon sample taken from the base level of the sparse gravelly clay unit covering the fault (ŞAH-11) is $10,422 \pm 37$ years. Calendar age is 10,646–10,149 BC. (Figure 20). Detailed information is provided under the title paleoseismological interpretation. This fault trends NE-SW, cutting across the E-W trending Bozkurt segment and indicating that the Dazkırı segment is older than the Bozkurt segment. This is further confirmed by the age data from the base level of the overlying sediment.

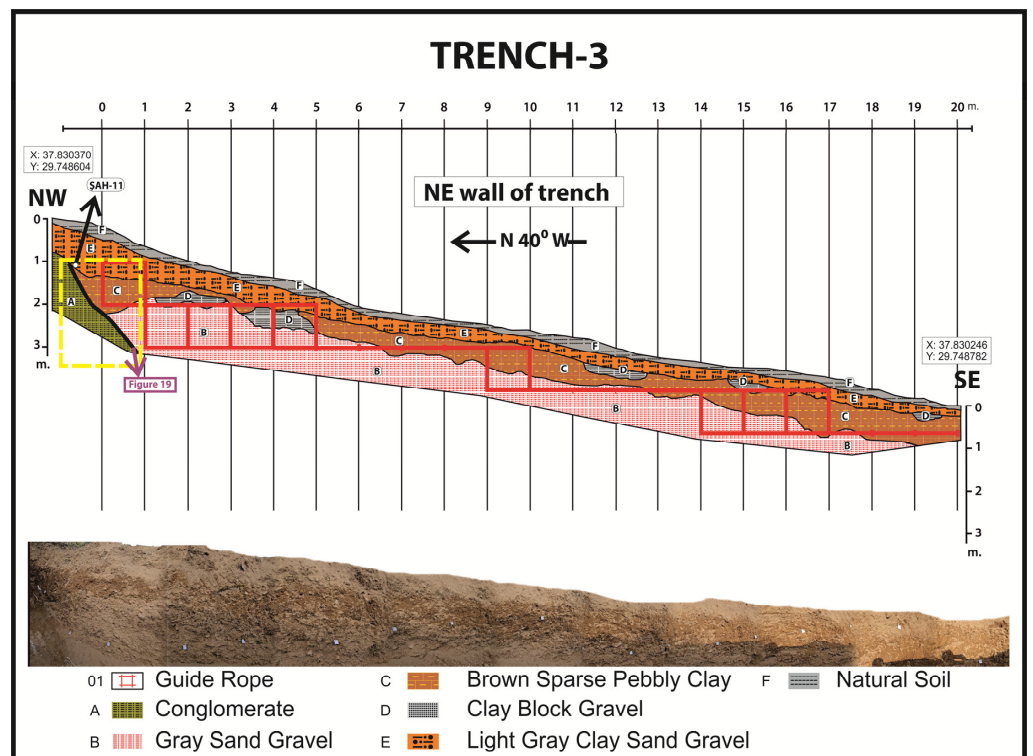


Figure 18. View of Trench-3 and the geological cross section on the NE wall of the trench.

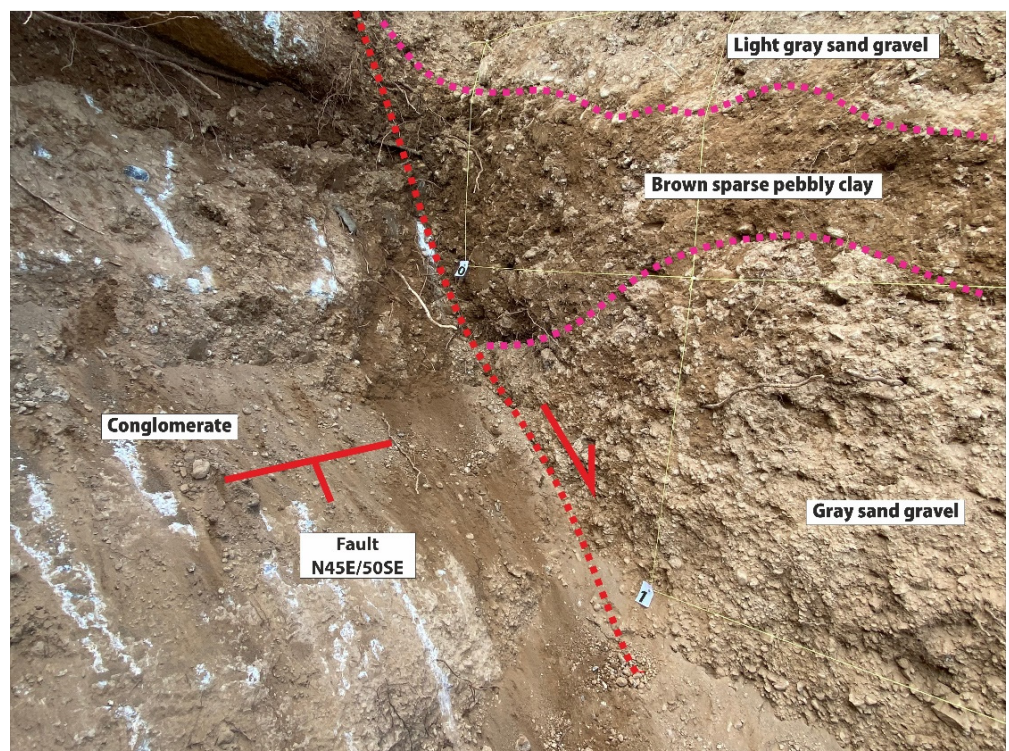


Figure 19. Fault mirror and lithological levels observed at the NW end of Trench-3.

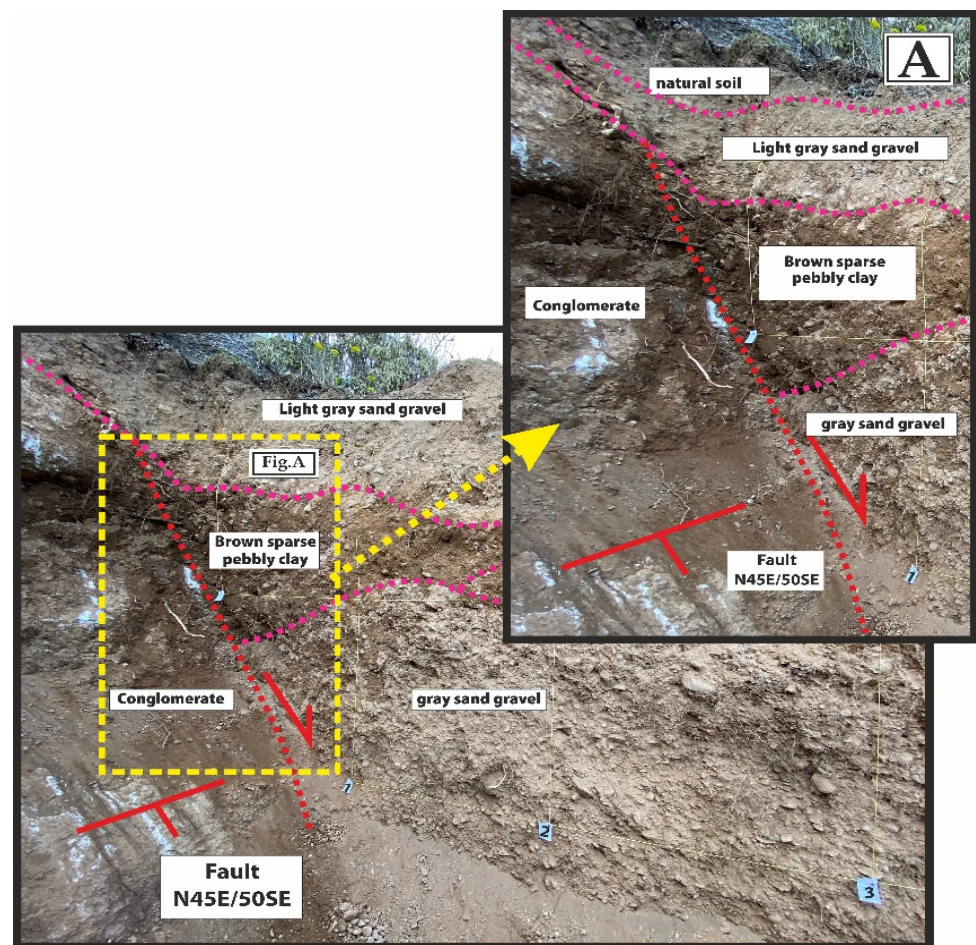


Figure 20. Distant and close view of lithologies from 0–3 m from NW inside Trench-3 (View towards N). A: A close look at the fault plane in trench 3.

3. Summary of Paleoseismological Observations

The Maymundağı fault zone, forming the northern boundary of the Acıgöl graben, consists of the NE-SW trending Dazkırı segment extending approximately 13 km to the east and the E-W trending Bozkurt segment approximately 17 km long to the west. Paleoseismological investigations were conducted at two separate trenches in the middle sections of the likely younger Bozkurt segment to the west. In Trench-1, excavated 15 m to the west, two distinct fault zones were identified. A minor slip was observed in the NE observed fault zone, while a larger slip and different lithological levels were noted along the fault zone in the middle of the trench. Thus, the zone with greater slip is interpreted as the main fault zone. Data indicate that fault segments within this zone were active in two separate periods in the past. A fault segment north of the zone, which is approximately 1.5 m wide, was covered by Unit F. A segment located a few centimeters south of the same fault cut Unit F, generating a 42 cm dip slip. This fracture was also covered by Unit G above. Radiocarbon dating from the base level of Unit F (sample ŞAH-8) provided an age of 1322 years, while the base level of Unit G (sample ŞAH-7) offered an age of 598 years. The displacement measured here was 42 cm, suggesting an earthquake-generating surface rupture occurred within 724 years, with an estimated slip rate of 0.58 mm/year.

Additionally, the earthquake's magnitude, based on the [42] equation, is estimated to be around $M = 6.5$ (Figure 21). Although the discussed segment covers an area of about 17 km in the study area, the surface rupture length should be between 23 and 24 km, according to the Wells and Coppersmith graph. As a result, surface ruptures resulting from separate earthquakes that occurred approximately 598 years ago and 1322 years ago developed in the same region. Based on these data, the calibrated calendar range of

the earthquake, which occurred approximately 1322 years ago, is 655–774 A.D, while the calibrated calendar range of the earthquake, which subsequently occurred approximately 598 years ago, is 1304–1405 A.D.

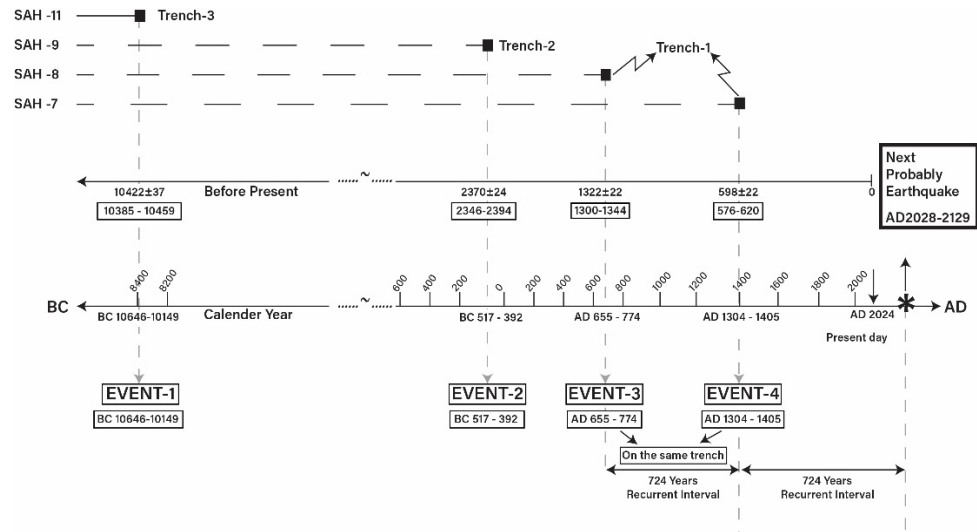


Figure 21. Radiocarbon-based distribution diagram of possible earthquakes that may occur in the Maymundağı fault zone. Dating analysis of Şah-7 and Şah-8 samples taken in Hendek-1, Şah-9 sample taken in Hendek-2, and Şah-11 sample taken in Hendek-3 (calibration date and radiocarbon date) 3. (Detailed explanations are included in the text under the Section 3).

The age of the ^{14}C sample taken from Trench-1 opened on the eastern flank of the Maymundağı fault zone, provides the closest age data we have to the present day. Based on data obtained from the trenches, this fault ruptured approximately 598 years ago, and its calibrated calendar age is 1304–1405 AD. When the calculated 724-year recurrence period is added to the calibrated calendar years, it can be predicted that this fault may produce an earthquake again in the future between 2028 and 2129 AD. However, these data may not be sufficient for a sound interpretation.

Approximately 2 km of Trench-1 was opened on the E-W trending Bozkurt segment, and Trench-2 was opened on the same fault zone where the fault was detected. The age of the radiocarbon sample taken from the base level of Unit D, which covers the fault, is 2370 years (ŞAH-9). At this location, the fault was dated approximately 2370 years ago, corresponding to the calibrated calendar date of 517–392 BC. Since no other fractures or age analyses were detected in the trench, it is difficult to make paleoseismological interpretations.

The Dazkırı segment, eastward of the Maymundağı fault zone, is oriented NE-SW, contrasting with the westward Bozkurt segment-oriented E-W. While the fan deposits accumulated significantly ahead of the Bozkurt segment, the same deposits in front of the Dazkırı segment are less. Despite the clear fault linearity in morphology, no data on fault linearity were observed on the stiff conglomerates at the base block.

Therefore, the NE-SW trending segment may have occurred in the period before the E-W trending segments. The same circumstances exist south of the graben. For the seismic history of the Dazkırı segment, Trench-3 was opened, and the fault zone was identified. Trench-3, which was opened in a location that is close to the SW end of the NE-SW oriented zone to the east of Trench-2, presents a structure just like Trench-2.

The C-14 age analysis of the sample (ŞAH-11) obtained from the base level of Unit E, which covers the fault at the SW end of the trench, indicates that an earthquake capable of causing surface rupture occurred 10,422 years ago.

This suggests that the NE-SW trending segment may have been activated earlier than the E-W trending segment. Moreover, characteristic features such as fault slickenlines on the NE-SW trending segment have disappeared over a long period (Table 1).

Table 1. Results of the radiocarbon date analysis (TUBITAK Marmara Research Center) (National Electrostatics Corporation, Model 3SDH-1 (UAMS)) [43,44].

No	Trench Name	Sample Number	Lab ID Number	Material Type	Radiocarbon Age (BP)	2 Sigma Calibration
1	TRENCH-1	ŞAH-7	TÜBİTAK-3361	Sediment	598 ± 22	68.3% probability 1320 (56.7%) 1359 calAD 1389 (11.6%) 1398 calAD 95.4% probability 1304 (74.2%) 1366 calAD 1383 (21.1%) 1405 calAD
2	TRENCH-1	ŞAH-8	TÜBİTAK-3362	Sediment	1322 ± 22	68.3% probability 660 (38.9%) 683 calAD 745 (23.9%) 760 calAD 767 (5.5%) 772 calAD 95.4% probability 655 (54.5%) 705 calAD 738 (41.0%) 774 calAD
3	TRENCH-2	ŞAH-9	TÜBİTAK-3363	Sediment	2370 ± 24	68.3% probability 466 (24.4%) 436 calBC 422 (43.8%) 395 calBC 95.4% probability 571 (95.4%) 392 calBC
4	TRENCH-3	ŞAH-11	TÜBİTAK-3365	Sediment	10422 ± 37	68.3% probability 10,629 (3.4%) 10,611 calBC 10,534 (13.1%) 10,611calBC 10,443 (3.6%) 10,611 calBC 10,409 (10.8%) 10,611calBC 10,359 (17.6%) 10,611calBC 10,287 (18.2%) 10,611calBC 10,165 (1.6%) 10,611 calBC 95.4% probability 10,646 (8.4%) 10,593 calBC 10,542 (16.3%) 10,470calBC 10,459 (70.7%) 10,149calBC

4. Discussion and Conclusions

The study area is situated between the NE-SW trending Burdur and Çivril-Baklan grabens, east of Denizli, in western Anatolia, Turkey. The S-SE boundary of the graben is defined by the Gemiş fault zone, while the N-NW boundary is bounded by the Maymundağı fault zone.

In the central part of the Acıgöl graben, intra-basin faults trend approximately E-W. The Maymundağı fault zone consists of the eastward NE-SW trending and dipping towards the SE Dazkırı segment and the westward E-W trending dipping towards the south Bozkurt segment.

There is a lack of detailed studies investigating past earthquakes on the Maymundağı fault zone, resulting in a significant gap in the literature concerning its tectonic evolution and seismic characteristics. Therefore, this study primarily focuses on the seismic history of the Maymundağı fault. To address this, paleoseismological investigations were conducted on the two segments of the fault zone oriented in different directions.

It was observed that sedimentary fan deposits accumulated ahead of the westward Bozkurt segment, composed of several fractures, whereas the younger sedimentary fan deposits accumulated ahead of the eastward Dazkırı segment, consisting of a single fracture. Additionally, although fault scarps and lineaments were observed on the Dazkırı segment, no fault gouges were observed on the fault mirror. In contrast, fault gouges were clearly observed on the Bozkurt segment to the west.

It can be suggested that the eastern Dazkırı segment of the Maymundağı fault zone was active at least 10,422 years ago, and subsequently, earthquakes migrated westward, concentrating on the westward E-W trending segments. In later periods, a rejuvenation towards the west was observed within the E-W trending segments in terms of their potential for generating earthquakes.

It can be stated that while an earthquake occurred 2370 years ago in the eastern region of the E-W trending segment, movements occurred first 1322 years ago and then 598 years ago on the same segment towards the west.

Particularly, the recurrence interval of earthquakes that caused surface ruptures at two different times in the same trench can be suggested as an average of 724 years.

Considering that the last historical earthquake on this fault occurred 598 years ago, which corresponds to the calibrated year range of 1304–1405 AD, it can be predicted that the next earthquake on the same fault may occur between 2028 and 2129 AD. These findings are important for understanding the seismic history of the region. It is important to conduct paleoseismological studies in the region in order to add new data to the data obtained in this study and to make more precise interpretations.

Author Contributions: Conceptualization, Ş.K. and M.H.; methodology, M.H.; software, Ş.K.; validation, Ş.K. and M.H.; formal analysis, Ş.K.; investigation, M.H.; resources, Ş.K.; data curation, M.H.; writing—original draft preparation, Ş.K.; writing—review and editing, M.H.; visualization, Ş.K.; supervision, M.H.; project administration, Ş.K.; funding acquisition, M.H. All authors have read and agreed to the published version of the manuscript.

Funding: This study was supported by the Pamukkale University Scientific Research Project (Project No: 2024HZDP001).

Institutional Review Board Statement: Not applicable.

Informed Consent Statement: Not applicable.

Data Availability Statement: The original contributions presented in the study are included in the article, further inquiries can be directed to the corresponding author.

Acknowledgments: This study includes a portion of the research initiated by Şahali Kaya as part of his doctoral dissertation and continued with detailed studies on the side faults of the Acıgöl graben. We thank all the referees who evaluated this study during the manuscript stage and provided constructive comments and suggestions. I would like to thank Erdal Akyol and Hıdır Gümüş for his critical criticism and assistance.

Conflicts of Interest: The authors declare no conflicts of interest.

References

- Erinç, S. Die Morphologischen Entwicklungstadien der Küçük Menderes-Masse. *Rev. Geogr. Inst. Univ. Istanbul* **1955**, *2*, 93–95.
- McKenzie, D. Active Tectonics of the Alpine-Himalayan Belt: The Aegean Sea and Surrounding Regions. *Geophys. J. R. Astron. Soc.* **1978**, *55*, 217–254. [[CrossRef](#)]
- Şengör, A.M.C. The North Anatolian Transform Fault: Its Age, Offset, and Tectonic Significance. *Geol. Soc. Sp.* **1979**, *136*, 269–282. [[CrossRef](#)]
- Şengör, A.M.C.; Yılmaz, Y. Tethyan Evolution of Turkey: A Plate Tectonic Approach. *Tectonophysics* **1981**, *75*, 181–241. [[CrossRef](#)]
- Yılmaz, Y.; Genc, S.C.; Gurer, O.F.; Bozcu, M.; Yılmaz, K.; Karacık, Z.; Altunkaynak, Ş.; Elmas, A. When Did the Western Anatolian Grabens Begin to Develop? *Geol. Soc. Sp.* **2000**, *173*, 353–384. [[CrossRef](#)]
- Ambraseys, N.N.; Tchalenko, J.S. Seismotectonic Aspects of the Gediz, Turkey, Earthquake of March 1972. *Geophys. J. R. Astron. Soc.* **1972**, *30*, 229–252. [[CrossRef](#)]
- Eyidoğan, H.; Jackson, J.A. A Seismological Study of Normal Faulting in the Demirci, Alaşehir, and Gediz Earthquakes of 1969–70 in Western Turkey: Implications for the Nature and Geometry of Deformation in the Continental Crust. *Geophys. J. R. Astron. Soc.* **1985**, *81*, 569–607. [[CrossRef](#)]
- Westaway, R. Neogene Evolution of the Denizli Region of Western Turkey. *J. Struct. Geol.* **1993**, *15*, 37–53. [[CrossRef](#)]
- Taymaz, T.; Price, S. The 1971 May 12 Burdur Earthquake Sequence, SW Turkey: A Synthesis of Seismological and Geological Observations. *Geophys. J. Int.* **1992**, *108*, 589–603. [[CrossRef](#)]
- Jackson, J.; McKenzie, D. Rotational Mechanisms of Active Deformation in Greece and Iran. *Geol. Soc. Lond. Sp. Publ.* **1984**, *17*, 743–754. [[CrossRef](#)]
- Ambraseys, N.N. Engineering Seismology. *J. Earthq. Eng. Struct. Dyn.* **1988**, *17*, 51–105. [[CrossRef](#)]
- Yılmaztürk, A.; Burton, P.W. Earthquake Source Parameters as Inferred from the Body Waveform Modeling, Southern Turkey. *J. Geodyn.* **1999**, *27*, 469–499. [[CrossRef](#)]
- Nyst, M.; Thatcher, W. New Constraints on the Active Tectonic Deformation of the Aegean. *J. Geophys. Res.* **2004**, *109*, 23. [[CrossRef](#)]
- Över, S.; Pinar, A.; Ozden, S.; Yılmaz, H.; Unlugenc, U.C.; Kamacı, Z. Late Cenozoic Stress Field in the Cameli Basin, SW Turkey. *Tectonophysics* **2010**, *492*, 60–72. [[CrossRef](#)]
- Catlos, E.J.; Ertel, T.M.; Cemen, I. *Extensional Tectonics in Western Anatolia: Eastward Continuation of the Aegean Extension*; AGU Books: Kayseri, Turkey, 2021. [[CrossRef](#)]
- Hancer, M. Geological Evidences Belonging to Late Holocene Seismic Activity in the South of Denizli Graben (Southwestern Turkey, Southeastern European Part). *Carpath. J. Earth Environ. Sci.* **2019**, *14*, 137–153. [[CrossRef](#)]
- Elitez, İ.; Yaltrak, C.; Aktuğ, B. Extensional and Compressional Regime Driven Left-Lateral Shear in Southwestern Anatolia (Eastern Mediterranean): The Burdur-Fethiye Shear Zone. *Tectonophysics* **2016**, *688*, 26–35. [[CrossRef](#)]
- Emre, O.; Duman, T.Y.; Ozalp, S.; Elmacı, H.; Olgun, Ş.; Şaroğlu, F. *Active Fault Map of Turkey in 1:1,250,000 Scale*; Maden Tetkik ve Arama Genel Müdürlüğü Özel Yayınlar Serisi–30: Ankara, Turkey, 2013. (In Turkish)
- Şengör, A.M.C. Cross-Faults and Differential Stretching of Hanging Walls in Regions of Low-Angle Normal Faulting: Examples from Western Turkey. *Geol. Soc. Lond. Sp. Publ.* **1987**, *28*, 575–589. [[CrossRef](#)]
- Seyitoğlu, G.; Scott, B. Late Cenozoic Crustal Extension and Basin Formation in West Turkey. *Geol. Mag.* **1991**, *128*, 155–166. [[CrossRef](#)]
- Seyitoğlu, G.; Scott, B.C.; Rundle, C.C. Timing of Cenozoic Extensional Tectonics in West Turkey. *J. Geol. Soc.* **1992**, *149*, 533–538. [[CrossRef](#)]
- Bozkurt, E. Neotectonics of Turkey—A Synthesis. *Geodin. Acta* **2001**, *14*, 3–30. [[CrossRef](#)]
- Altunel, E.; Barka, A.; Akyüz, S. Paleoseismicity of the Dinar Fault, SW Turkey. *Terra Nova* **1999**, *11*, 297–302. [[CrossRef](#)]
- Ambraseys, N.N.; Finkel, C.F. *The Seismicity of Turkey and Adjacent Areas: A Historical Review, 1500–1800*; M.S. Eren: Istanbul, Turkey, 1995.
- Sözbilir, H.; Eski, S.; Tepe, Ç.; Duran, İ.; Özkaymak, Ç.; Tiryakioğlu, İ.; Doğan, O.; Akyar, E.B. *8 Ağustos 2019 Kuşadası Körfezi (İzmir) ve Bozkurt (Denizli) Depremleri Özet Raporu*. DEÜ ve Kocatepe Üniversitesi Deprem Araştırma ve Uygulama Merkezi, 19 s. 2019. Available online: https://daum.deu.edu.tr/wp-content/uploads/2019/08/izmir_denizli_deprem_raporu_DUAM_DAUM.pdf (accessed on 14 January 2023).
- Emre, O.; Duman, T. *Simav-Kütahya Earthquake (Mw: 5.8) in Turkey Pre-Assessment, Earthquake Report*; General Directorate of Mineral Research and Exploration (MTA), Earth Dynamics Research Center: Ankara, Turkey, 2011. (In Turkish)
- Helvacı, C.; Alçiçek, M.C.; Gündoğan, İ.; Gemici, Ü. Tectonosedimentary Development and Palaeoenvironmental Changes in the Acıgöl Shallow-Perennial Playa-Lake Basin, SW Anatolia, Turkey. *Turk. J. Earth Sci.* **2013**, *22*, 173–190. [[CrossRef](#)]
- Alçiçek, H. Late Miocene Nonmarine Sedimentation and Formation of Magnesites in the Acıgöl Basin, Southwestern Anatolia, Turkey. *Sediment. Geol.* **2009**, *219*, 115–135. [[CrossRef](#)]
- Göktaş, F.; Çakmakoglu, A.; Tari, E.; Sütçü, Y.F.; Sarıkaya, H. *Çivril-Çardak Arasının Jeolojisi*. M.T.A. Rap. No. 318. 1989. Available online: <https://dergipark.org.tr/tr/download/article-file/191367> (accessed on 18 July 2023).

30. Tagliasacchi, E.; Yağmurlu, F. Acıgöl Grabeni Kuzeyindeki Pliyo-Kuvaterner Yaşlı Karasal Çökellerin Fasiyes Özellikleri ve Bölgenin Paleootamsal Gelişimi, GB-Türkiye. *Süleyman Demirel Üniversitesi Fen Bilim. Enstitüsü Derg.* **2019**, *23*, 440–451. [[CrossRef](#)]
31. Koçyiğit, A.; Unay, E.; Saraç, G. Episodic Graben Formation and Extensional Neotectonic Regime in West Central Anatolia and the Isparta Angle: A Case Study in the Akşehir-Afyon Graben, Turkey. *Geol. Soc. Lond. Sp. Publ.* **2000**, *173*, 405–421. [[CrossRef](#)]
32. Koçyiğit, A.; Özacar, A.A. Extensional Neotectonic Regime through the NE Edge of the Isparta Angle, SW Turkey: New Field and Seismic Data. *Turk. J. Earth Sci.* **2003**, *12*, 67–90.
33. Koçyiğit, A. The Denizli Graben-Horst System and the Eastern Limit of Western Anatolian Continental Extension: Basin Fill, Structure, Deformational Mode, Throw Amount, and Episodic Evolutionary History, SW Turkey. *Geodin. Acta* **2005**, *18*, 167–208. [[CrossRef](#)]
34. Koçyiğit, A.; Deveci, Ş. A N–S-Trending Active Extensional Structure, the Şuhut (Afyon) Graben: Commencement Age of the Extensional Neotectonic Period in the Isparta Angle, SW Turkey. *Turk. J. Earth Sci.* **2007**, *16*, 391–416.
35. Koçyiğit, A. *Akgöl (Burdur) Grabeninin Neotektonik Özellikleri ve Kenar Faylarının Depremselliği*. Türkiye Bilimsel ve Teknik Araştırma Kurumu Çevre, Atmosfer Yer ve Deniz Bilimleri Araştırma Grubu. 2010. Available online: <https://open.metu.edu.tr/bitstream/handle/11511/50524/TVRJeU9EQXc.pdf> (accessed on 22 September 2024).
36. Gürboğa, Ş.; Koçyiğit, A. Yeni bir genişleme yapısı: Akgöl (Afyon-Burdur) güncel grabeni ve neotektonik-sismik özellikleri. In Proceedings of the 13th Aktif Tektonik Araştırma grubu konferansı, Çanakkale, Türkiye, 8–11 September 2009; pp. 24–25.
37. Emre, O.; Duman, T.Y.; Ozalp, S.; Olgun, S.; Elmaci, H. *1:250,000 Scale Active Fault Map Series of Turkey, Afyon (NJ 36-5) Quadrangle*; General Directorate of Mineral Research and Expansion (MTA): Ankara, Turkey, 2011.
38. Ege, İ.; Duman, N. Maymun Dağı (Çardak-Denizli/Dazkırı-Afyonkarahisar)'nın Morfotektonik Özelliklerinin CBS ile Belirlenmesi. *Turk. Stud. Soc.* **2020**, *15*, 277–307.
39. Kürçer, A.; Özdemir, E.; Uygun, G.C.; Duman, T.Y. The First Paleoseismic Trench Data from Acıpayam Fault, Fethiye-Burdur Fault Zone, SW Turkey. *Bull. Geol. Soc. Greece* **2016**, *50*, 75–84. [[CrossRef](#)]
40. Kaya, A. Mikrozonlama Bölgelerinde Paleosismolojik Araştırmalar: Çardak Örneği (Denizli, GB Türkiye). *Niğde Ömer Halisdemir Üniversitesi Mühendislik Bilim. Derg.* **2018**, *7*, 1113–1118. [[CrossRef](#)]
41. Ma, H.; Dong, S. A Case of Paleoseismic Evidence of Normal Fault Capable of Triggering an M> 8 Earthquake—Study on Sertengshan Range-Front Fault, North Margin of Hetao Basin, China. *J. Struct. Geol.* **2024**, *184*, 105145. [[CrossRef](#)]
42. Wells, D.L.; Coppersmith, K.J. New Empirical Relationships Among Magnitude, Rupture Length, Rupture Width, Rupture Area, and Surface Displacement. *Bull. Seism. Soc. Am.* **1994**, *84*, 974–1002. [[CrossRef](#)]
43. Doğan, T.; İlkmen, E.; Kulak, F. A New National 1 MV AMS Laboratory at TÜBİTAK MRC in Turkey. *Nucl. Instrum. Methods Phys. Res. Sect. B* **2021**, *509*, 48–54. [[CrossRef](#)]
44. Doğan, T.; İlkmen, E.; Kulak, F. Radiocarbon Analysis and Status Report from Türkiye: 1MV National AMS Laboratory (TÜBİTAK-AMS). *Radiocarbon* **2023**, *65*, 375–388. [[CrossRef](#)]

Disclaimer/Publisher's Note: The statements, opinions and data contained in all publications are solely those of the individual author(s) and contributor(s) and not of MDPI and/or the editor(s). MDPI and/or the editor(s) disclaim responsibility for any injury to people or property resulting from any ideas, methods, instructions or products referred to in the content.